GEOCHEMISTRY, MINERALOGY AND PETROLOGY • SOFIA
ГЕОХИМИЯ, МИНЕРАЛОГИЯ И ПЕТРОЛОГИЯ • СОФИЯ
2009, **47**, 109-133.

The Malko Tarnovo pluton in Southeastern Bulgaria: II. Evolution of the ore-magmatic system

Rossen Nedialkov, Borislav K. Kamenov, Bojidar Mavroudchiev, Eugenia Tarassova, Mitko Popov

Abstract. The Late Cretaceous Malko Tarnovo pluton (Strandzha Mountain, SE Bulgaria) is composed of 4 phases. The first three phases are result of the evolution of monzonitic magma, forming an isometric intrusive body, crystallized at 710-930°C and P = 4-7 kbar. The fourth porphyritic phase was intruded in shallower depth (P = 3 kbar), consolidated in E-W elongated bodies and crystallized at 700-810°C.

The magma source of monzonitoids is an enriched mantle, melted at low to moderate degree (5-10%), at water undersaturated conditions with residual rutile. The magma of the porphyritic phase was generated by deep crustal melting induced by hot mantle-derived magma. The magmatic evolution is dominated by fractional crystallization of clinopyroxene and to a lesser degree of magnetite, amphibole, olivine and plagioclase. Crustal contamination is weakly pronounced.

The water content of the monzonitoid magma is about 4.0-5.5 wt.%, and 3.5 to 5.5 wt.% for porphyritic magmas. The oxygen fugacity of the magmas is 1 to 1.5 units above the NNO buffer. The monzonitoid magma became water saturated at the end of the crystallization process (residual 30% of the intruded magma). Exsolved fluids are less mobile and form skarns and massive Cu-sulphide bodies. The porphyritic magma reaches water saturation at 45% of its crystallization and forms a porphyry type Cu-W-Mo mineralization.

Key words: Malko Tarnovo pluton, magmatic evolution, thermobarometry, ore-magmatic system

Addresses: R. Nedialkov, B.K. Kamenov, B. Mavroudchiev – Faculty of Geology and Geography, Sofia University "St. Kliment Ohridski", 1504, Sofia, Bulgaria; E-mail: rned@gea.uni-sofia.bg; E. Tarassova – Central Laboratory of Mineralogy and Crystallography, Bulgarian Academy of Sciences, 1113 Sofia, Bulgaria; M. Popov – Geological Institute, Bulgarian Academy of Sciences, 1113 Sofia, Bulgaria

Росен Недялков, Борислав К. Каменов, Божидар Маврудчиев, Евгения Тарасова, Митко Попов. Малкотърновският плутон, Югоизточна България: II. Еволюция на рудно-магматичната система

Резюме. Горнокредният Малкотърновски плутон (Странджа, ЮИ България) е съставен от 4 фази. Първите три са резултат от развитието на монцонитоидна магма и изграждат едно приблизително изометрично тяло, кристализирало при 710-930°C и налягане от 4-7 килобара. Четвъртата, порфиритова фаза е внедрена на по-плитко ниво (P = 3 kbar), кристализирала е при 700-810°C и изгражда удължени в И - З посока дайкоподобни тела.

Източникът за монцонитоидната магма е обогатена мантия като топенето е с нисък до умерен процент (5-10%) при водонедонаситени условия и остатъчен рутил в източника. Магмата, образувала порфиритовата фаза е свързана с топене на долната кора при въздействието на гореща мантийна

магма. Магматичната еволюция е доминирана от фракционирането на клинопироксен и в по-малка степен на магнетит, амфибол, оливин и плагиоклаз. Коровата контаминация е по-слабо проявена.

Водното съдържание на монцонитоидната магма е около 4-5,5 тегл.%, а за порфиритовата то е 3,5-5,5 тегл.%. Фугитивността на кислорода на магмите е 1 до 1,5 единици над NNO буфер. Монцонитоидната магма става водонаситена към края на своята кристализация (при около 30% остатъчна топилка). Отделилите се флуиди са по-слабо подвижни и образуват скарновия ореол и масивните медно-сулфидни тела. Порфиритовата магма достига водонаситено състояние, когато е изкристализирала 45% и е в основата на образуването на Cu-W-Mo порфирна минерализация.

Introduction

Repeatedly target of various investigations from different points of view, the Malko Tarnovo pluton outcrops in Strandzha Mountain and is of key significance for clearing up of the geological evolution of the area. As one of the ore-magmatic centers in the Eastern Bulgaria, it attracted the attention of many regional geologists, tectonists, petrologists and metallogenists. The pluton was intruded into Triassic sequences of the Lipachka and Malko Tarnovo Formations and within Lower Jurassic sedimentary rocks (Chatalov 1980, 1985, 1990; Čatalov 1983). Several polymetallic skarn-type deposits are attached to the Malko Tarnovo Ore Field: Gradishte, Propada and Mladenovo, as well as the Mo-Cu porphyry deposit Bardtse (Vassileff et al. 1964; Bonev & Yordanov 1983).

The present paper follows the previous one of Kamenov et al. (2006) devoted to the geological position, petrography and mineralogy of the Malko Tarnovo pluton. It aims tracing back the geochemical evolution of the magmatism and deducing of the petrological processes, leading to the formation of the ore-magmatic system.

The former metallogenic studies of the area had drawn attention mainly to the chemistry of the magmatic products and to its geochemical specialization. According to Vassileff & Stanisheva-Vassileva (1981, 1986) the Cu-Au-polymetallic vein and skarn-type ore formation is genetically related predominantly to intermediate and transitional in alkalinity magmatism, whereas the porphyry copper formation originated from intermediate to acid calc-alkaline magmatism, showing weak potassic tendency. Ignatovski et al. (1986) advanced the idea that the porphyry copper deposits and occurrences within the Strandzha Zone are related not only to the calc-alkaline magmatism, but also to the transitional in alkalinity magmatism (Prohorovo and the Zidarovo porphyry deposits).

Geology

The Malko Tarnovo pluton is multistage differentiated body composed of several consequently intruded phases. Recent studies of our team (Mavroudchiev[1] et al. 1996; Kamenov et al. 2000, 2006) consider the pluton as built up by 4 magmatic phases: (1) basic; (2) monzonitoid; (3) quartz-syenitic; (4) acid porphyry rocks (Fig. 1). The rocks of these phases are clearly outlined spatially and distinguished by cutting relationships. The first three phases form a relatively isometric body. The rocks of the fourth phase were intruded at different tectonic and strain field, forming bodies elongated in subequatorial direction. Several rock varieties with gradual transitions were demarcated in each of the phases (Kamenov et al. 2006).

The plutonic exposures on Bulgarian territory cover an area of 12 km^2. The outcrops in Turkish territory are approximately 6 km^2, but the rocks there are not studied in details. The Derekoy intrusive body (Aykol & Tokel

[1] Mavroudchiev B, Kamenov B, Nedialkov R, Tarassova E, Iliev Z, Petrov P, Iliev R. 1996. Final report of the investigations of the contract № 8б1996 "Temporal and lateral evolution of the gold-generating role of the Malko Tarnovo pluton from Eastern Srednogorie, with respect to metallogenic estimations. Geoarchive of the Ministry of Environment and Water (in Bulgarian)

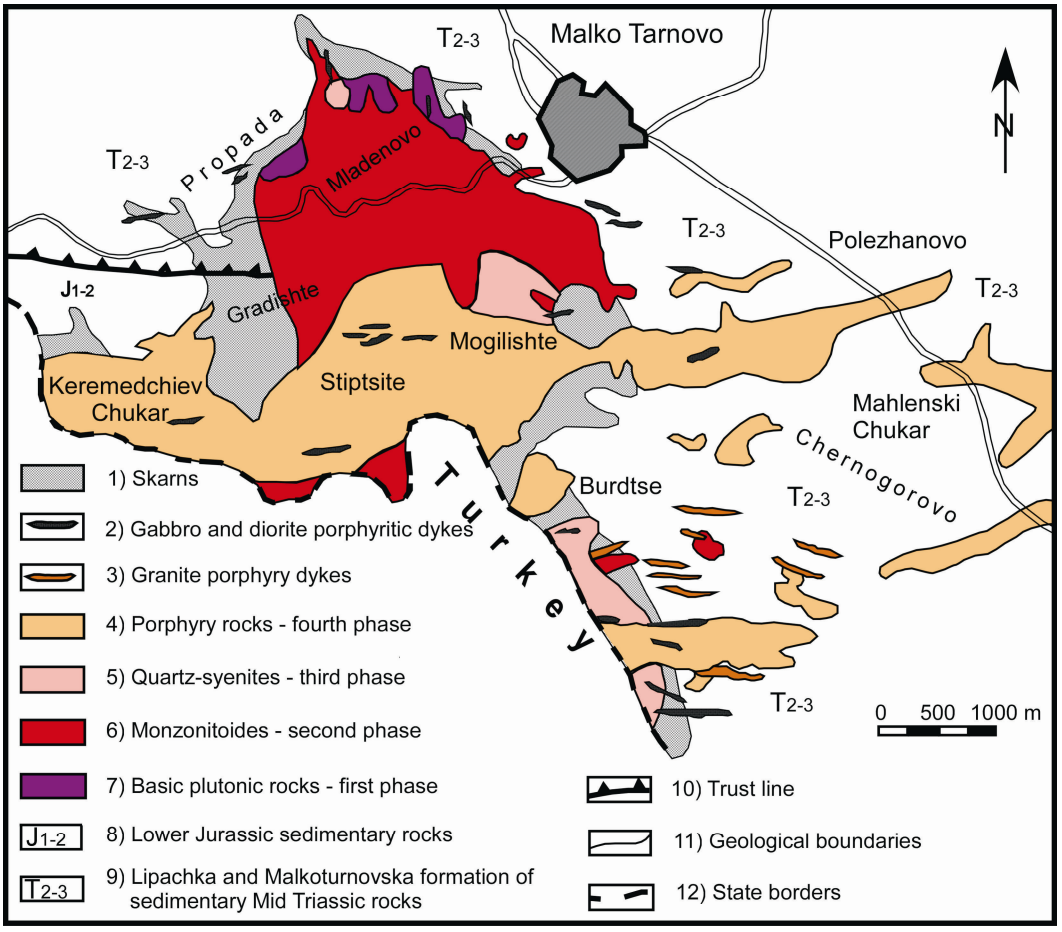

Fig. 1. Geological sketch map of the Malko Tarnovo pluton

1991) having similar petrographical and chemical composition occurs in close neighborhood at a distance of about 15–20 km southeast.

The Malko Tarnovo pluton was dated (Kamenov et al. 2000) in Late Cretaceous time demonstrating some age divergence for its phases (74-76 Ma for gabbro and quartz-monzonite samples and 66 Ma for granodiorite porphyry).

The intrusion of the magmatic bodies has given rise to appearing skarns into the country rocks and formation of hornfelses on the terrigenous alumosilicate rocks. The magnesian (diopside-forsterite) skarns are developed after dolomitized marbles in the magmatic stage. The calcic skarns (garnet-pyroxene) are infiltration- and diffusion-related ones, formed upon calcite limestones and marbleized limestones (Vassileff et al. 1964; Staykov 1972). Hydrothermal ore mineralization is superimposed on the skarns with development of quartz, chlorite, calcite and sulphides. The ore bodies represent zones or steep dipping pillar-like bodies, containing the following types of ores: magnetite, magnetite-chalcopyrite; chalcopyrite-specularite, chalcopyrite, bornite, chalcopyrite-molybdenite-scheelite (Bogdanov 1987). The Gradishte, Propada and Mladenovo deposits are mainly of magnetite-chalcopyrite skarn type (Bogdanov 1987), while the deposit

Bardtse, localized in the southeastern part of the Malko Tarnovo pluton within the porphyry acid rocks of the fourth phase is predominantly disseminated vein type Cu-Mo deposit and vein quartz-Mo one (Bonev & Yordanov 1983). All these deposits are included into the Malko Tarnovo Ore Field.

Brief petrographical characteristics of the Malko Tarnovo pluton

The following four plutonic phases were described in details in a preceding paper (Kamenov et al. 2006).

The first, basic (gabbro-pyroxenite) phase consists of 3 small bodies in the northern marginal part of the pluton, having altogether a common area of less than 1 km^2. The gabbro rocks are the prevailing variety in this phase. Three plagioclase generations with varying composition are distinguished in these rocks.

The second, monzonitoid phase covers the central part of the pluton. It is the most widespread equigranular rock variety including monzodiorite, quartz-monzodiorite, monzonite and quartz-monzonite. Micrographic eutectic texture of the felsic minerals occurs in some rare cases, supervened on the crystallization of the pyroxenes and the other mafic minerals.

The third, quartz-syenitic phase occupies separate spots within the monzonitoids. The rocks of this phase are exposed in the central, as well as in the southern and the northern parts of the pluton. The rock varieties are amphibole-biotite and biotite-amphibole quartz-syenites and monzogranites.

The fourth phase of the acid porphyry rocks is composed of quartz-diorite porphyry, granodiorite porphyry, quartz-monzonite porphyrites and quartz-syenite porphyry. A great variety of bodies with different size and shape occur in elongated, East-West orientated outcrops. The rocks are massive, usually mezzo- to leucocratic, having porphyritic texture, suggesting shallower level of their crystallization. Phenocrysts represent up to 45% of the rocks. Micrographic quartz-feldspar intergrowths occur in the fine-grained matrix, disclosing the water saturation character of their magma. The essential minerals of the matrix are K-feldspar, quartz and plagioclase, rarely–some mafic minerals.

Petrology

Petrochemistry and geochemistry

The petrochemical peculiarities of the Malko Tarnovo pluton are deduced from 103 major element and 89 trace element (89-XRF and 37-AAA) analyses (Tables 1 and 2). Nine out of them are taken from the paper of Vasileff et al. (1964), 37 are from unpublished data of Svetla Yossifova (performed in the Laboratory for Geological Prospecting and Geochemical Analyses, Geological Survey) and 57 are done in the Chemical Laboratory of the Faculty of Geology and Geography (classical wet analysis) during our study.

The values of SiO_2 range between 42 and 73 wt.%. On the classification plot SiO_2 *vs.* (Na_2O+K_2O) (Fig. 2), the samples fall within the fields of pyroxenite, gabbro, monzodiorite, monzonite, quartz-diorite, quartz-monzonite, granodiorite, syenite and quartz-syenite. The rocks from the first three phases are referred entirely to the high-K type magmatic rocks (transitional in alkalinity series). On the same plot, the rocks from the fourth phase are medium-K to mainly high-K type with alkalinity clearly lower than that in the monzonitoids (Fig. 3). The cumulative rocks (gabbro-pyroxenites and pyroxenites) of the first phase are distinguished by their low alkalinity.

The rocks of the first three phases are assigned to the shoshonite series in the K_2O *vs.* SiO_2 diagram (after Peccerillo & Taylor 1976 - not shown here), whereas the ones from the fourth phase are related to the high-K calc-alkaline series. The cumulative rocks of the first phase fall in the low-K (tholeiitic) to medium-K (calc-alkaline) series.

The main part of the basic first phase consists of olivine- and hypersthene-normative rocks. About 20% out of them are quartz-normative. All of the rest rocks are quartz-

Table 1. *Major elements (in wt.%) and CIPW normative mineral composition of the rocks from the Malko Tarnovo pluton*

Sample No	102	127a	119i	1/92	119e	119z	123	101	U/92	131	135	119k	132b	111	2/92
Rock	Pxt	Pxt	Gb	Gb	Md	Mz	Mz	QMz	QMz	QSy	QSy	QSy	QDp	QMzp	QSyp
Phase	I	I	I	I	II	II	II	II	II	III	III	III	IV	IV	IV
SiO_2	44.37	50.97	47.70	49.13	55.59	54.40	55.77	58.67	59.90	66.52	66.42	66.59	60.70	60.97	67.97
TiO_2	0.45	0.67	0.68	1.29	0.89	0.65	0.62	0.39	1.01	0.35	0.75	0.60	0.46	0.41	0.77
Al_2O_3	15.33	13.67	10.67	15.24	15.00	12.20	16.20	16.56	16.63	14.23	14.53	15.38	15.70	17.47	15.36
Fe_2O_3	2.35	2.09	6.21	4.56	3.28	4.12	4.08	3.00	2.80	1.06	2.95	1.68	2.25	1.10	1.86
FeO	3.24	4.29	6.49	6.46	5.36	4.09	3.31	3.38	3.43	2.95	1.30	1.70	5.62	2.96	1.94
MnO	0.09	0.12	0.18	0.16	0.13	0.18	0.17	0.18	0.10	0.13	0.13	0.18	0.08	0.10	0.05
MgO	7.19	6.89	12.50	8.11	4.45	4.05	3.75	3.00	3.25	1.71	1.73	1.30	2.25	2.23	0.78
CaO	22.93	16.84	9.98	8.78	6.90	7.33	7.09	6.10	5.09	4.46	2.88	1.93	4.30	6.63	2.97
Na_2O	0.62	2.21	1.70	2.75	2.94	3.29	3.69	3.77	3.45	2.95	3.43	3.20	3.10	4.34	3.34
K_2O	0.02	0.31	1.30	2.41	3.73	4.46	3.76	4.19	3.93	4.65	5.19	6.66	2.63	2.77	3.98
P_2O_5	2.32	0.88	0.70	0.58	0.92	0.67	0.64	0.30	0.60	0.12	0.08	0.01	0.18	0.19	0.18
H_2O^-	0.05	0.17	0.40	0.09	0.12	0.04	0.12	0.09	0.08	0.09	0.03	0.11	0.35	0.51	0.12
H_2O^+	0.66	0.43	1.18	0.02	0.44	0.17	0.41	0.07	0.13	0.17	0.40	0.36	1.90	0.56	0.29
Total	99.62	99.63	99.70	99.57	99.75	99.65	99.61	99.70	100.00	99.68	99.82	99.70	99.52	100.24	99.61
A/CNK	0.35	0.39	0.47	0.65	0.70	0.51	0.70	0.76	0.87	0.99	0.88	0.89	0.79	0.88	0.96
CIPW norms															
Q	0.00	1.74	0.00	0.00	5.19	2.56	3.15	5.13	10.25	19.93	19.13	16.29	16.97	8.81	25.91
Or	0.12	1.83	7.68	14.24	22.04	26.36	22.22	24.76	23.22	27.48	30.67	39.36	15.54	16.37	23.52
Ab	5.25	18.70	14.38	23.27	24.88	27.84	31.22	31.90	29.19	24.96	29.02	27.08	26.23	36.72	28.26
An	38.99	26.46	17.64	22.12	16.72	5.35	16.54	15.89	18.28	11.85	8.92	7.93	20.16	20.01	13.56
Di	45.08	40.06	21.64	14.11	9.33	21.34	11.49	9.03	2.44	7.85	3.77	1.28	0.00	9.54	0.00
Hy	0.00	2.80	19.79	4.14	12.46	3.23	5.89	6.05	9.43	4.57	2.56	3.17	13.45	4.92	2.79
Ol	0.00	0.00	5.06	11.17	0.00	0.00	0.00	0.00	0.00	0.00	0.00	0.00	0.00	0.00	0.00

(Pxt) pyroxenite;(Gb) gabbro; (Md) monzodiorite; (Mz) monzonite; (QMz) quartz-monzonite; (QSy) quartz-syenite; (QDp) quartz diorite porphyry; (QMzp) quartz-monzonite porphyry; (QSyp) quartz-syenite porphyry. Data is from wet chemical analysis

Table 2. *Trace elements (in ppm) of the rocks from the Malko Tarnovo pluton*

Sample №	102	127a	119i	1/92	119e	119z	123	101	U/92	131	135	119k	132b	111	2/92
Rock	Pxt	Pxt	Gb	Gb	Md	Mz	Mz	QMz	QMz	QSy	QSy	QSy	QDp	QMzp	QSyp
Phase	I	I	I	I	II	II	II	II	II	III	III	III	IV	IV	IV
V $_{XRF}$	90	100	200		110	220	150	130		50	110	40	40	200	
Cr $_{AAA}$	62	197	900	325	127	84	52	77	41	109	34	41	212	87	26
Ni $_{AAA}$	35	7	264	161	54	22	27	35	22	24	16	16	59	23	16
Co $_{AAA}$	20	31	46	50	25	21	21	20	12	12	16	15	12	14	8
Cu $_{AAA}$	32	193	26	121	92	312	118	110	105	388	57	34	102	31	65
Pb $_{AAA}$	3	5	5	5	12	27	14	12	13	5	288	398	11	19	10
Zn $_{AAA}$	98	42	465	430	76	92	80	88	52	43	35	188	46	53	181
Zr $_{XRF}$	62	157	557		234	222	339	354		99	290	706	66	225	
Y $_{XRF}$	18	23	25		43	53	64	45		31	27	31	28	42	
Nb $_{XRF}$	5	7	5		16	26	34	21		15	20	36	9	19	
Ba $_{XRF}$	30	160	340		630	610	640	630		620	600	990	2530	500	
Sr $_{AAA}$	54 1	502	900	566	401	449	434	400	224	335			401	501	119
Rb $_{AAA}$	48	45	126	95	240	236	247	212	294	116	130	140	162	171	485
Li $_{AAA}$	8	19	12	12	14	10	16		21				37	6	

Rock abbreviations as in Table 1. (XRF) X-ray fluorescence; (AAA) atomic absorption analysis

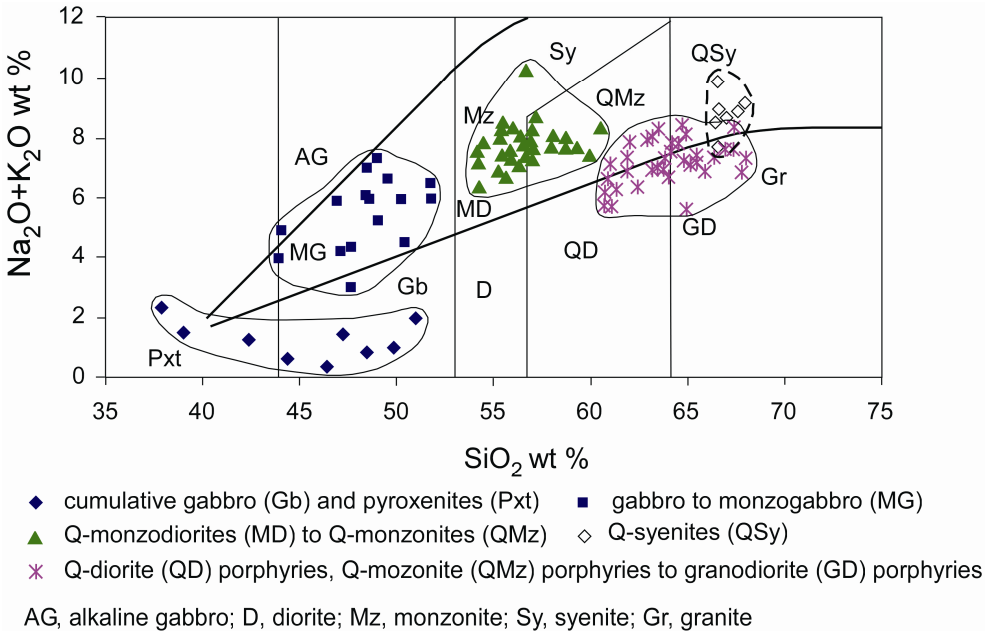

Fig. 2. SiO_2 *vs.* (Na_2O+K_2O) classification diagram (after Bogatikov et al. Eds. 1983) for the rocks of the Malko Tarnovo pluton

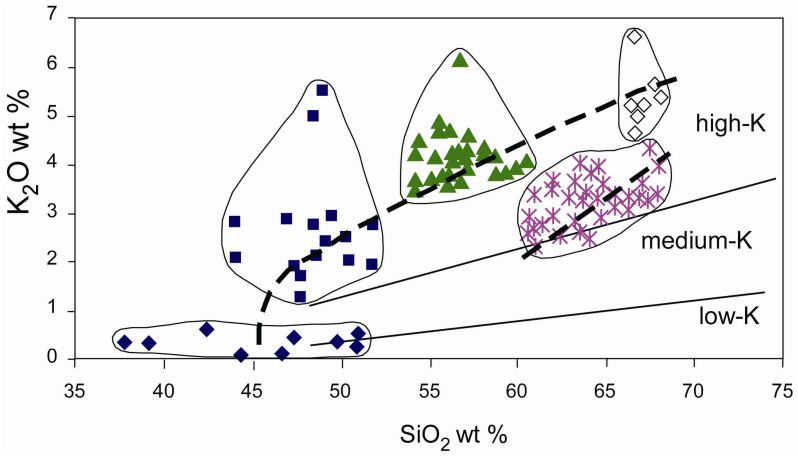

Fig. 3. SiO_2 *vs.* K_2O diagram (after Le Maitre et al. 1989) for the magmatic series in the Malko Tarnovo pluton. Dashed lines show the trends of the magmatic evolution. Symbols as in Fig. 2

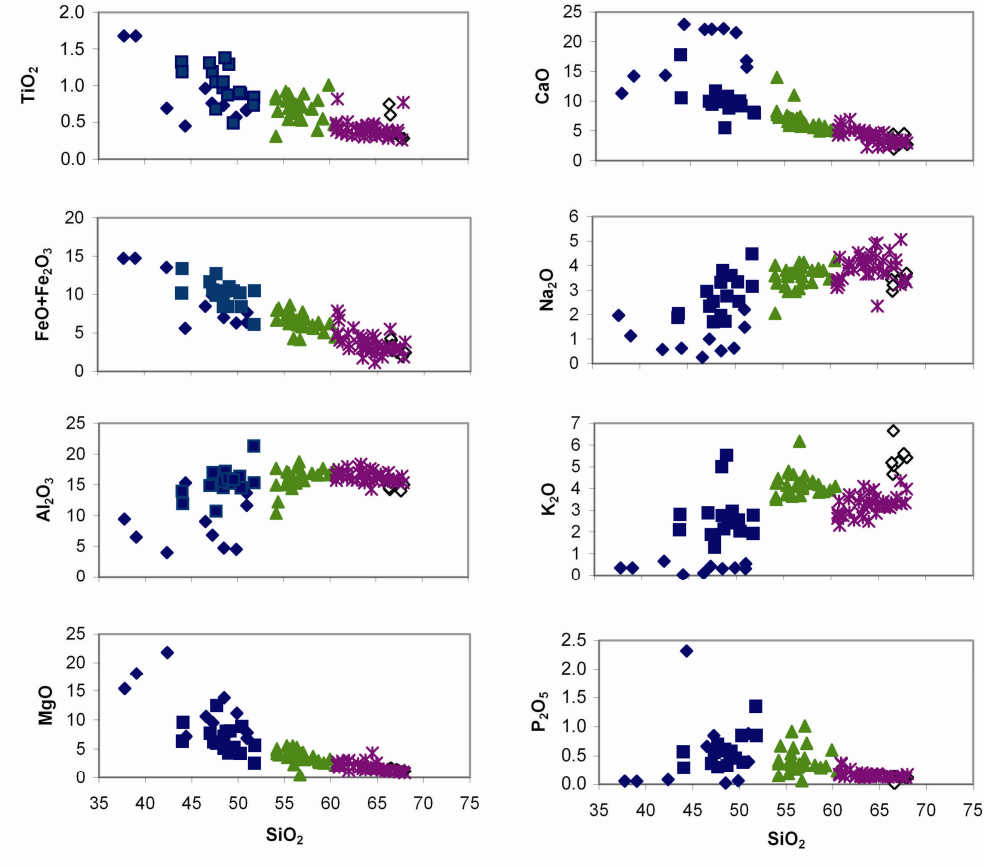

Fig. 4. Harker diagrams for the major oxides (in wt.%) of the Malko Tarnovo plutonic rocks. Symbols as in Fig. 2

normative and the only exception is some single samples of monzodiorites, which are olivine-normative.

Harker's oxide and element diagrams (Figs. 4, 5) of all sequences revealed increasing of the concentrations of Na_2O, K_2O, Rb, Zr, Y, Nb and decreasing of MgO, CaO, $FeO+Fe_2O_3$, TiO_2, Ni, and Co. At the same time, the monzonitoid and porphyry rocks exhibit clearly different trends for the variations of K_2O, Rb, Zr, Cu, Y, and Nb. On the background of some similarities, there are important compositional differences between the rocks of the first three phases on one side and the porphyry rocks from the fourth phase, on the other. This means that both groups of rocks are broadly consistent with different evolutional processes. Comparing the petrochemical and geochemical characteristics of gabbroids from the first phase with the cumulative rocks, we ascertain the fact that the last rocks are remarkable for their higher contents of CaO and MgO and lower contents of Al_2O_3, K_2O, Na_2O, TiO_2, Zn, Ba, Sr, Rb, Nb, V, and Y. The clinopyroxene as their main rock-forming constituent should be the principal fractionating mineral during the magmatic differentiation.

The cumulative nature of the pyroxenites is demonstrated clearly on the diagram Co *vs*. K_2O (Fig. 6). The monzonitoid differentiated pluton (first to third phases) could be drawn from a parental basic melt through a process of mineral fractionation. Regardless of the fact that some samples from the porphyry rocks of the fourth phase fall within the main trend of chemical evolution, it is obvious that they form their own specific subtrend, which is discrepant from the main trend.

Chondrite-normalized spectra are characterized by *LREE*-enrichment compared to *HREE* and by clearly expressed negative Eu-anomaly (Fig. 7 and Table 3). The fractionation factor $(La/Yb)_n$ increases with the progress of the magmatic evolution in the monzonitoids. Thus, it is 3.8-8.0 for the basic rocks of the first phase, 8.0-11.7–for the monzonitoids of the second phase and up to 12.9 – for the quartz-syenites of the third phase. This factor ranges 9.5-15.3 in the porphyry granitoids.

The negative Eu anomaly for the samples of the first three phases is in the range 0.31-0.44 and no characteristic differences are established for these rocks. Contrary, this anomaly is visibly weaker for the samples of the porphyry granitoids: 0.47-0.60. A possible explanation for the Eu anomaly, even at the most primitive basic rock varieties, might be related to the parental magma source bearing plagioclase, which had not been melted or had been melted partially, or to early (preceding the intrusion of the first phase) plagioclase fractionation. An analytical decrease of the values of Eu cannot be excluded also. The relatively similar level of the Eu anomalies from the first to the third phase demonstrates that probably the fractionation of plagioclase was weakly expressed. A sum of the *REE* increases from the pyroxenites (114 ppm), through the gabbro (204-344 ppm) and to the monzonitoids (340-382 ppm), but is lower for the quartz-syenites of the third intrusive phase (209 ppm), where probably a fractionation of accessory minerals or fluid exsolution from the magma after the formation of the second, monzonitoid phase has been also realized. Radically different is this sum in the porphyry rocks from the fourth phase (143-214 ppm), which is another argument for their different origin and evolution path.

Trace elements of gabbro samples from the most primitive melts of the studied magmatic sequence (SiO_2 = 44-50.4%; MgO = 6-12.5%) plotted on FMM-normalized spidergrams (Fig. 8) after Pearce & Parkinson (1993) show very high values for the very highly incompatible elements (VHI), high values for the highly incompatible elements (HI) and comparatively lowest values for the moderately incompatible elements (MI). The negative Ti-anomalies on these plots correspond exactly to the theoretically deduced melts, obtained at weak to moderate melting degree (5-10 %) from an enriched mantle. A primordial mantle-normalized extended plot of a gabbro sample

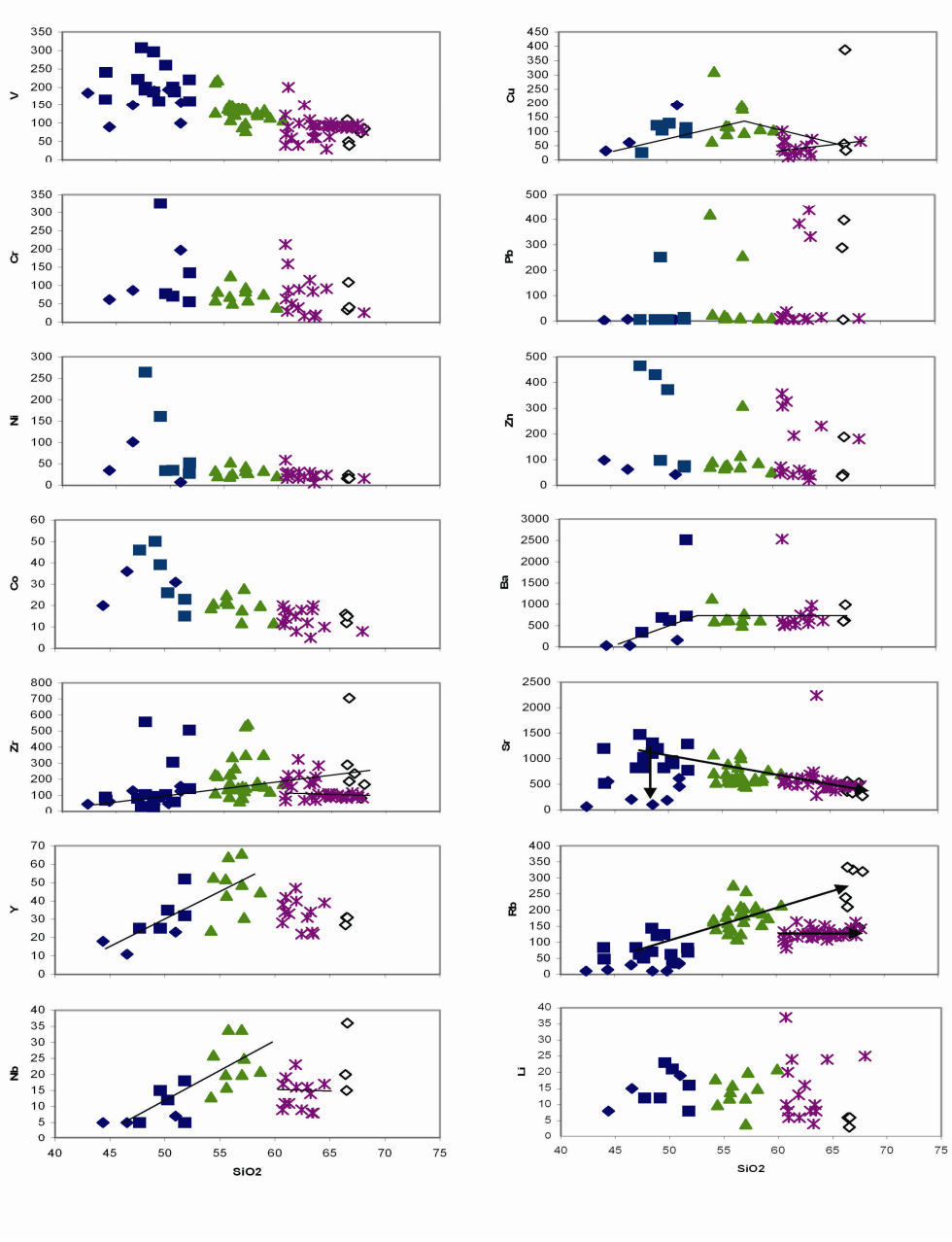

Fig. 5. Harker diagrams for trace elements (in ppm) of the Malko Tarnovo plutonic rocks. Oblique lines show the well defined trends of evolution. Symbols as in Fig. 2

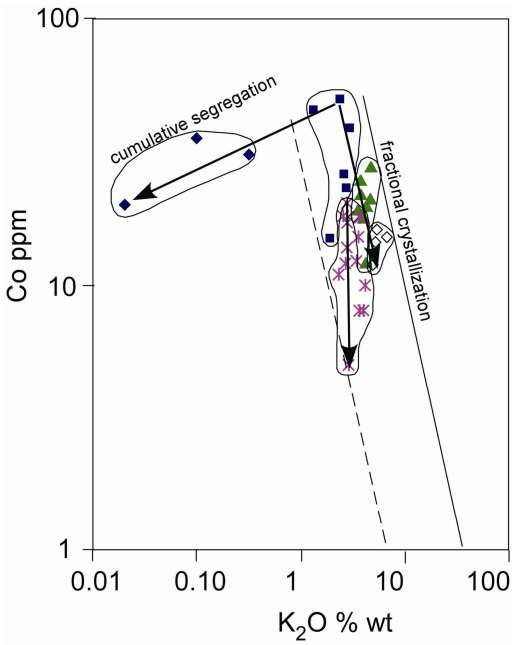

Fig. 6. Co *vs.* K_2O diagram (after Cocherie 1986) for the Malko Tarnovo plutonic rocks. The trends for the cumulative rocks (pyroxenites and gabbros) and the mineral fractionation differentiated rocks are well distinguished. The arrows show the trends related to different magmatic processes. Symbols as in Fig. 2

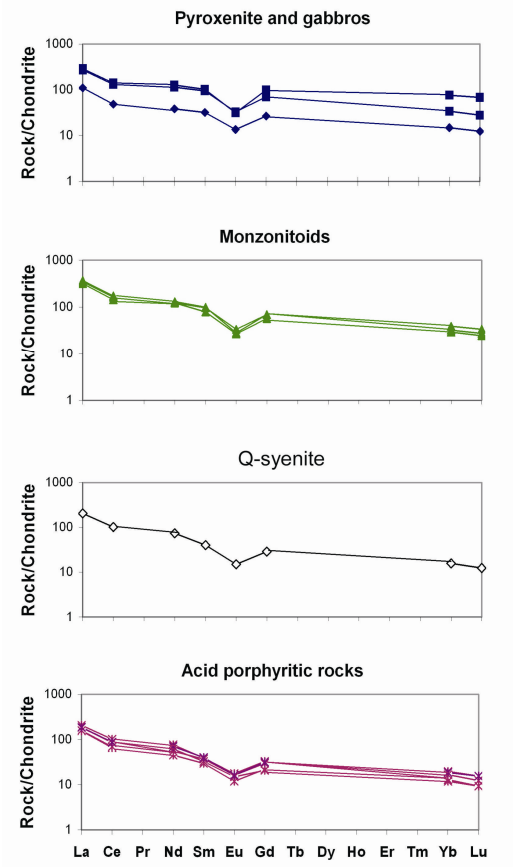

Fig. 7. Chondrite normalized patterns of the rare earth elements for the rocks of the Malko Tarnovo pluton. Normalizing values after Boynton (1984). Symbols as in Fig. 2

displays the typical for the island magmatic arcs distributions with their negative Nb- and Ti-anomalies (Fig. 9).

Modeling of the magmatic evolution

The mutually related mineralogical, petrochemical and geochemical variations in the rocks from the Malko Tarnovo pluton suggest ideas for the leading significance of a fractional crystallization process. Mathematical modeling of such process may assist to confirm many of the assumptions followed from the analysis of the various variation diagrams, as well as, from the textural relationships of the minerals. The strong correlations of FeO, Fe_2O_3, CaO, MgO, and K_2O with SiO_2 could be interpreted as a result of a fractionation of mineral association of mafic minerals and plagioclase. The mafic association, possibly contained olivine and orthopyroxene on an equal level with the clinopyroxene. The coordinated variations of V, Ti, Fe, and Mn suggest a fractionation of titanomagnetite and ilmenite. The combined look at the distributions of Rb, together with the one of V emphasizes also the hornblende as a likely participant in the fractionation. All these assumptions are checked by the applied simple mixing model (Le Maitre 1979) used.

Table 3. *REE content from rocks of the Malko Tarnovo pluton (in ppm)*

Sample №	102	119j	3a	119z	100	101	131	130	106	111	127a	132a
Rock	Pxt	Gb	Gb	Mz	Mz	Sy	QSy	QDp	QDp	QMzp	QMzp	QSyp
Phase	I	I	I	II	II	II	III	IV	IV	IV	IV	IV
La	34	84	89	99	115	108	63	64	48	49	57	58
Ce	39	105	113	117	141	132	82	82	53	56	69	71
Nd	23	68	76	75	79	74	44	46	27	33	37	42
Sm	6.2	18.3	19.9	19.1	19.5	15.6	7.8	7.6	5.8	7.2	6.4	7.8
Eu	1.0	2.4	2.3	2.5	2.1	2.0	1.1	1.3	0.88	1.2	1.1	1.2
Gd	6.9	18.1	25.4	18.1	18.1	15.0	7.5	8.5	5.7	7.7	5.4	8.2
Yb	3.1	7.1	15.8	8.3	6.8	6.2	3.3	4.1	2.7	3.5	2.5	3.9
Lu	0.4	0.9	2.2	1.1	0.9	0.8	0.4	0.5	0.3	0.4	0.3	0.5
Total	113.6	303.8	343.6	340.1	382.0	353.6	209.1	214.0	143.4	158.0	178.7	192.0
La/Yb	7.4	7.97	3.79	8.05	11.4	11.7	12.9	10.5	12.0	9.46	15.3	10.0
Eu/Eu*	0.49	0.41	0.31	0.43	0.35	0.40	0.44	0.48	0.47	0.51	0.60	0.47

Rock abbreviations are as in Table 1. Samples are analyzed with ICP-AES by L. Alexieva (Eurotest, Sofia)

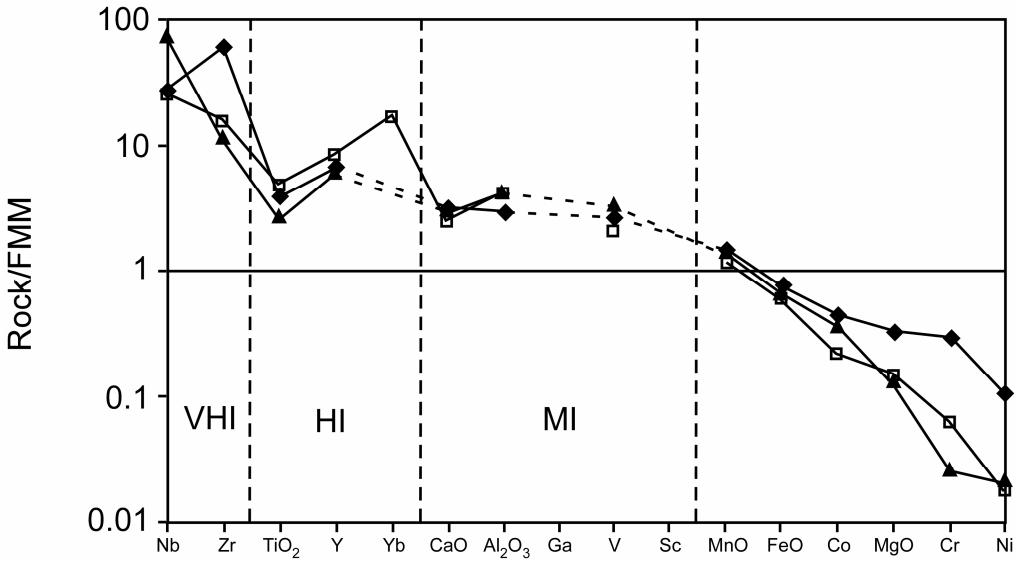

Fig. 8. Fertile MORB Mantle (FMM) normalized spidergrams for gabbro: the most primitive igneous rocks of the pluton, after Pearce & Parkinson (1993). (VHI) very highly incompatible elements; (HI) highly incompatible; (MI) moderately incompatible

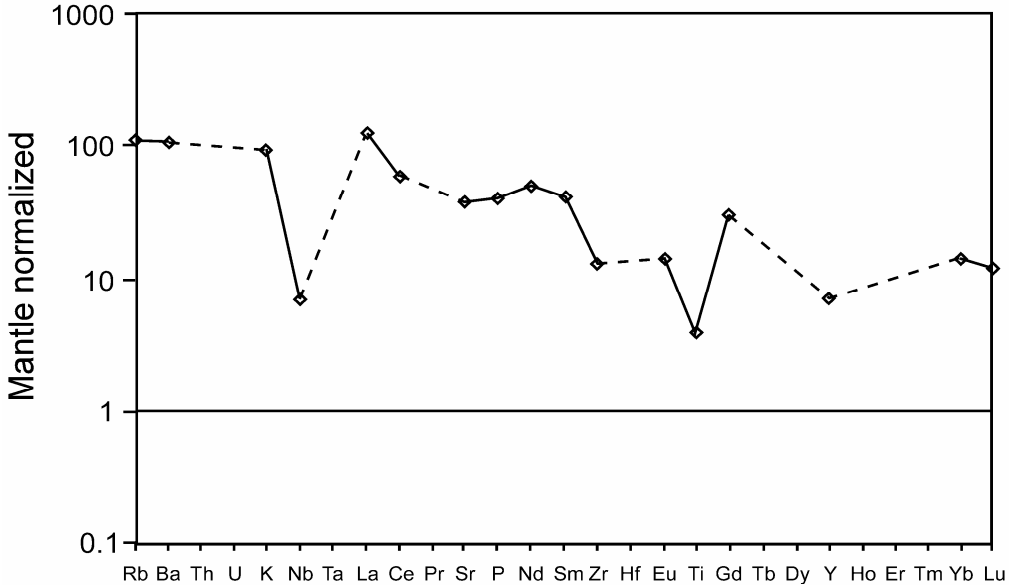

Fig. 9. Primordial mantle normalized spidergrams for gabbro from the Malko Tarnovo pluton (normalization values from Sun & McDonought 1989)

It is well portrayed by the following equation: $C_o = C_i.x_i + x_{dif}. C_{dif}$,
where C_o, C_i, and C_{dif} are the oxide contents in the initial parental magma, in the fractionating minerals and in the differentiated partial magma, respectively, while $x_i \ldots x_n$ are the weight proportions for each one of the separating mineral phases, and x_{dif} is the proportion of the differentiated and mathematically obtained melt. The problem for the estimation of the modal composition of the rock, when its bulk chemical composition is known has been resolved through the adapted by A. Andreev program GENMIX (Le Maitre 1979). The program gives a measure for the success of the modeling: the differences between the distances of the initial and the modeled compositions control the divergence between the theoretical and experimental compositions. The modeling is carried out in steps by selection of representative for the compositional range pairs of rock samples and acceptable petrologically fractionating mineral associations. Microprobe data of rock-forming minerals from the same rocks are used. Here, we selected for illustration only several out of the numerous trials with low values of $R = \sqrt{D^2}$, where D is the distance between the real and the modeled compositions in the space of the selected number of variables (major oxides).

The mathematically deduced trend of the compositional variations within the frames of SiO_2 *vs.* Na_2O+K_2O diagram is demonstrated in Fig. 10. It coincides comparatively well with the real compositional trend (Fig. 2). The used rock compositions in the modeling are specified in Table 4. In all equations above-stated and in the table, the rocks participating in the fractionation are abbreviated as follows: (Pxt) pyroxenite; (MGb) monzogabbro; (Gb) gabbro; (Mz) monzonite; (QMz) quartz-monzonite; (QSy) quartz-syenite; (QDp) quartz-diorite porphyrite; (GDp) granodiorite

A. Derivation of a cumulative pyroxenite from gabbro magma:
MGb_8: (11.5% Ol + 39.3% Pl + 6.0% Mt + 3.5% Ilm + 14.2% KFd) = 25.4% Pxt_{12}……. (1)
D=1.16

B. Obtaining of the extent of the internal differentiation within the gabbro field:
MGb_8: (7.6% CPx + 4.1% Mt + 29.8% Pl + 13.1% Ol + 2.1% Ilm + 19.0% KFd) = 29.3% Gb_{10}……. (2)
D=0.63
MGb_8: (3.3% Ol + 2.9% CPx + 9.6% Pl + 3.2% Mt + 0.7% Ilm) = 80.3% Gb_{15}……... (3)
D=0.93

C. Derivation of monzonitoids from gabbro magma:
MGb_8: (13.8% Ol + 11.1% CPx + 31.7% Pl + 4.7% Mt + 3.9% Ilm) = 34.9% Mz_{31}……. (4)
D=1.78
MGb_8: (1.25% Pl + 41.0% Hb + 7.5% Bt + 2.8% Mt + 1.0% Ilm) = 46.4% Mz_{31}……. (5)
D=1.04
Gb_{15}: (3.3% Pl + 43.0% Hb + 0.02% Mt + 1.72% Ilm) = 52.0% Mz_{29}……... (6)
D=1.80

D. Derivation of quartz-syenite from monzonitic magma
Mz_{29}: (32.4 % Pl + 38.5 % Hb + 20 % Bt + 8.1 % Cpx + 0.9 % Ap) = 52% QSy_{119k}……... (7)
D=1.96%

E. Derivation of granodiorite porphyry from quartz-diorite porphyritic magma–extent of the internal differentiation within the porphyry rocks field:
QDp_{130}: (54 % Pl + 37.2 % Hb + 8.8 % Mt) = 61.2 % GDp_{20-1}…….. (8)
D=1.79%

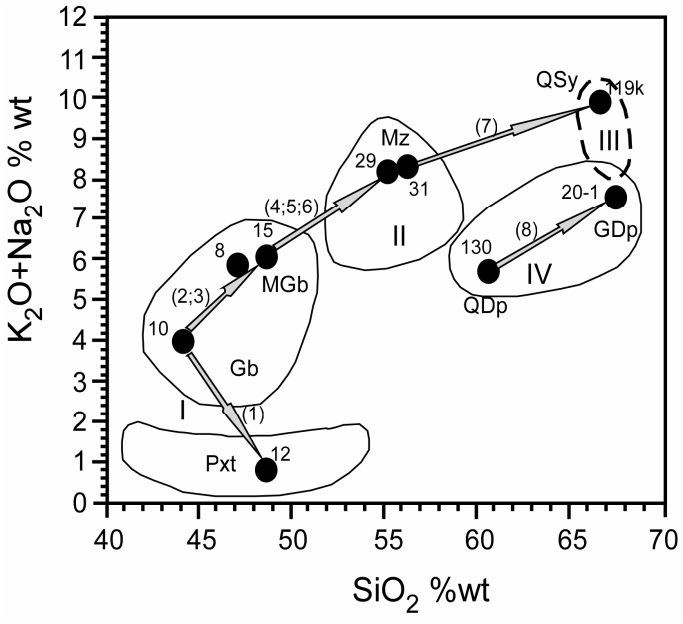

Fig. 10. Graphic representation of the calculated magmatic evolution model. Numbers close to spots are the numbers of the used analyses; numbers in parentheses are the successful model described in text

Table 4. *Rock compositions used for the magmatic evolution modeling of the Malko Tarnovo pluton*

Oxides Rocks	SiO_2	TiO_2	Al_2O_3	FeO_T	MnO	MgO	CaO	Na_2O	K_2O	P_2O_5	Total
Pxt_{12}	48.52	0.73	4.72	6.76	0.13	13.83	22.20	0.52	0.31	0.02	97.72
MGb_8	47.02	1.31	14.86	11.64	0.15	7.72	9.98	2.94	2.88	0.37	98.48
Gb_{10}	44.00	1.32	13.04	9.69	0.19	6.34	17.80	1.88	2.10	0.57	96.36
Gb_{15}	48.49	0.97	14.53	9.00	0.16	2.70	9.90	3.31	2.75	0.61	96.81
Mz_{31}	56.07	0.65	16.10	4.10	0.10	2.36	11.00	3.69	4.64	0.26	98.71
Mz_{29}	55.54	0.69	15.93	5.98	0.11	5.00	6.43	3.55	4.71	0.35	97.94
$QSy_{119к}$	66.59	0.60	15.38	3.14	0.18	1.30	1.93	3.20	6.66	0.01	98.98
QDp_{130}	60.91	0.43	16.72	7.12	0.10	1.78	5.94	3.40	2.31	0.36	98.71
$QDp_{20\text{-}1}$	67.35	0.39	15.42	1.63	0.02	1.34	3.25	3.22	4.36	0.15	97.22

Rock abbreviations are as in Table 1. Numbers after rock abbreviations are the numbers of the analyzed sample

porphyry. The subscripts are the serial numbers of the analyses. The used mineral abbreviations are the following: (Ol) olivine; (CPx) clinopyroxene; (Pl) plagioclase; (Mt) magnetite; (Ilm) ilmenite; (Hb) amphibole; (Bt) biotite; (KFd) K-feldspar; (Ap) apatite.

The successful modeling of the natural variations demonstrates that the fractionation from an initial parental composition, corresponding to the one of the samples Gb_{10} or MGb_8 step by step with consecutively decreasing total proportions of the fractionated minerals does not contradict to the empirically deduced compositional trend. Possible mixing between the acid and the basic magmas is another idea, which could be in line with the studied trend, the cumulative character of the pyroxenites and the mixed liquidus-solidus peculiarities of the most basic gabbro rocks. According to such process, the monzonitoids (third phase) might be equally derivative to the residual magma, after the separation of the association plagioclase, amphibole, clinopyroxene, magnetite and biotite from the parental gabbro magma, as well as a result of the mixing between acid and basic magmas. Some petrological and mineralogical criteria for disequilibrium in the rock-forming minerals (Kamenov et al. 2006) support the second idea, but convincing proofs for the eventual realization of such mechanism are to be sought only after specially designed sampling for isotope geochemistry. It is most likely that if there has been such a process at all, it probably had been realized on the background of the continuing simultaneously with the temperature variance fractional crystallization–the so called MFC process (mixing, fractionation, crystallization). The generation of quartz-syenite from quartz-monzonite magma (solution 7, modeling the transition between the second and the third phases), as well as of the granodiorite porphyry from quartz-diorite porphyry magma (solution 8, reproducing the internal differentiation in the porphyry rocks) require fractionation of significant quantities of plagioclase, which is most unlikely, according to the reading of the data. That put us in mind that the fractional crystallization has not been the only one process responsible for the magmatic evolution.

Tectonic setting

The applied tectonic discriminations supplement the conclusions from the geochemistry. On the diagram Rb *vs.* Y+Nb (Fig. 11) the acid rocks of the second, the third and the fourth phases fall in the fields of the island-arc and within-plate granitoid rocks. The crossing of some samples the within-plate granitoids field is probably due to the increased fluid activity of their magmas and also to their transitional alkalinity.

ORG-normalized spectra of monzonites and granodiorite porphyrites (Fig. 12) show the typical features of the island-arc magmatic

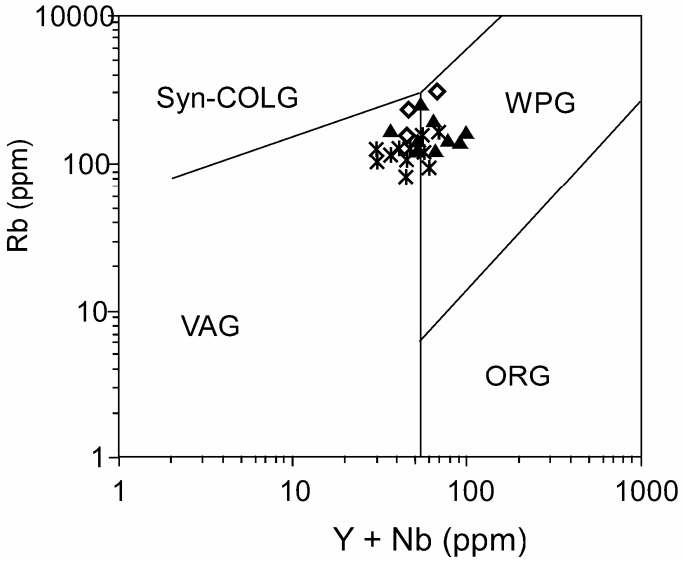

Fig. 11. Rb *vs.* (Y+Nb) discrimination diagram for the tectonic setting of granitoids (Pearce et al. 1984). (Syn-COLG) syn-collision granites; (VAG) volcanic arc granites; (WPG) within plate granites; (ORG) ocean ridge granites. Symbols as in Fig. 2

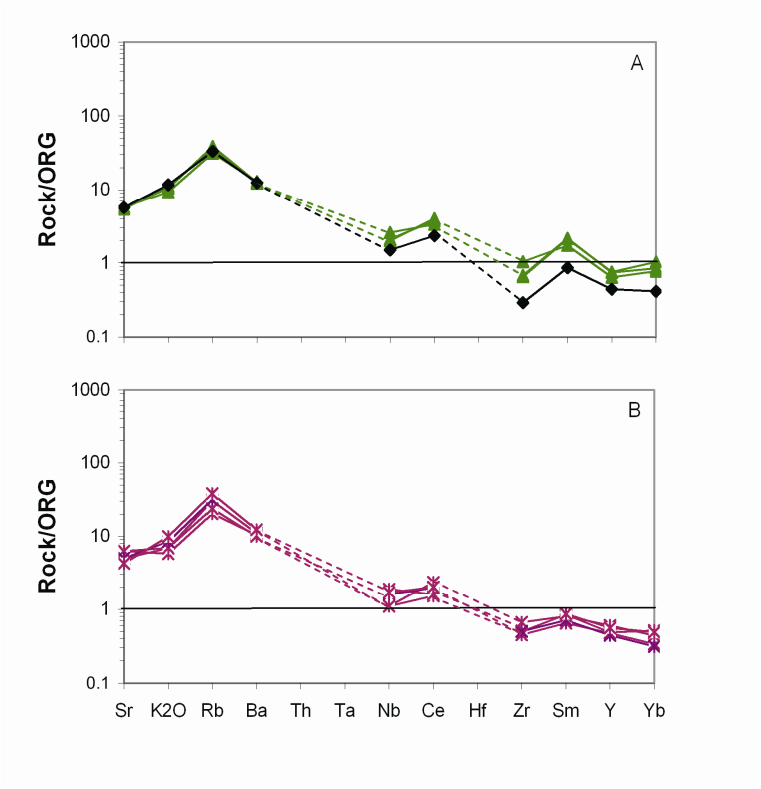

Fig. 12. ORG-normalized spidergrams for monzonitoids (A) and porphyritic rocks of the 4th intrusive phase (B) from the Malko Tarnovo pluton. ORG-normalization values are after Pearce et al. (1984)

rocks with their high values of LIL elements and the negative Nb and Zr anomalies. The porphyry rocks are distinguished from the monzonitoids by their lower values of HFSE and shallower negative anomalies.

All collected geochemical information evidences the subduction-related magmatism. The plot Rb/Zr *vs.* Nb (Fig. 13) assigns the studied rocks (equigranular and the later porphyry rocks, as well) to the normal continental arcs.

Isotope characteristics of the rocks

Strontium isotope data for the rocks of Malko Tarnovo were published earlier (Kamenov et al. 2000). The calculated ratio $^{87}Sr/^{86}Sr_i$ is in the range 0.7034-0.70691 for monzonitoids (corrected at 75 Ma age) and 0.7036-0.7038 (corrected at 66 Ma) for porphyry rocks (Fig. 14). The low ratio at the gabbro samples (0.7034) shows that they have experienced very weak influence of the crust material. The variations of this ratio in monzonitoids probably are due to the crustal contamination during the emplacement and solidifying of their magma at the background of an active fluid assistance. The rather low values of that ratio at the porphyry rocks suggest mantle origin for their parental magma or melts product of mantle derived rocks melting.

Estimated physical conditions of the magma evolution

The evaluation of physical parameters of the magma and the magmatic processes (evolution, cooling, and crystallization) as temperature, pressure, oxygen fugacity, water content, is very important for the characterization of the ore-magmatic system and for estimating its possible realization. Such evaluations for the temperature and pressure were made in the previous paper (Kamenov et al. 2006). Based on the zircon morphology (after Pupin 1980 and Pupin & Turco 1972) their temperature of crystallization in monzonitoids is in the range 900–750°C, and in the porphyry rocks: 730–600°C. The correlation between the amount of Al atoms in the site T_1O of the K-feldspars and the temperature at the end of the ordering process (Stewart & Wright 1974) is used to estimate the crystallization temperatures: 710–550°C. The low temperatures (under 650°C) were related to re-equilibration of the K-feldspars at relatively water-rich conditions. That is why the most of the estimated temperatures based on the two-feldspar thermometer (Furhman & Lindsley 1988) are also low (580-500°C). The application of the amphibole-plagioclase equilibration (Blundy & Holland 1990) gave the temperature of crystallization range 930-800°C for the gabbro and monzonitoids and 810-700°C for the porphyry rocks.

The estimated pressure of crystallization based on the Al content in the amphiboles (Johnson & Rutherford 1989) is 7-4 kbar (monzonitoids) and 4.2-2.5 kbar (porphyry rocks, started the phenocrysts solidifying in depth, before the final magma emplacement). The complete solidifying of the magma of the porphyry rocks probably has been realized at shallower levels of the Earth crust at lower pressures of the order of 2.5-3.0 kbar.

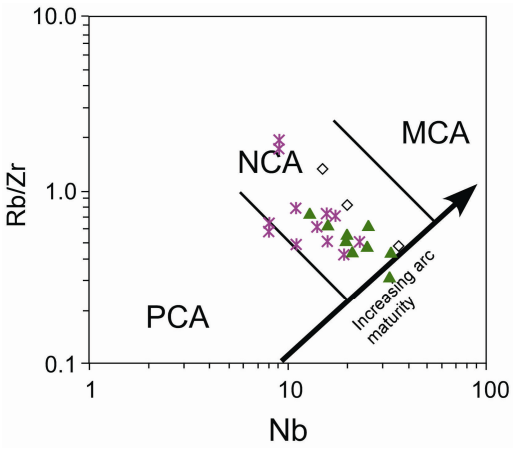

Fig. 13. Rb/Zr *vs.* Nb diagram for the arc maturity (after Brown et al. 1984). (PCA) primitive continental arc; (NCA) normal continental arc; (MCA) matured continental arc. Symbols as in Fig. 2

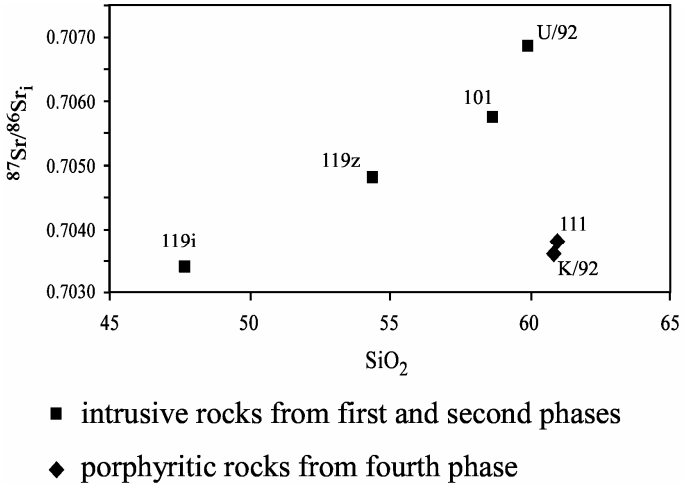

Fig. 14. $^{87}Sr/^{86}Sr$ *vs.* SiO_2 diagram for the rocks of the Malko Tarnovo pluton. Plot indexes correspond to the sample numbers in Table 1. (■) monzonitoids (first and second phases), (♦) porphyritic rocks

The magnetites and ilmenites also have been re-equilibrated in postmagmatic conditions at temperatures below 500°C (Kamenov et al. 2006) and at oxygen fugacity below HM buffer. The oxidizing conditions of crystallization can be estimated roughly by the application of the Wones & Eugster (1965) method from the biotite compositions, analyzed by wet chemical analyses of monomineral separates (Fig. 15). All analyzed biotites from monzonitoids fall between the buffers HM and NNO, but closer and to 1–2 units below the former. Biotites from the porphyry rocks fall immediately below the HM buffer. Compared to the monzonitoids, the porphyry rocks crystallized at shallower level at higher oxidation conditions.

A more precise estimation of the oxygen fugacity could be obtained with the titanite-magnetite-quartz paragenesis in the rocks. The method is suggested by Wones (1989) because late-stage re-equilibrations in calc-alkaline granitoides change the composition of magnetite and ilmenite and hamper the temperature and oxygen fugacity estimations. This was just the case in the Malko Tarnovo pluton. The estimated fugacity at the corresponding temperatures is 1 to 1.5 units above NNO buffer (Fig. 16). Such estimations are a bit lower than those

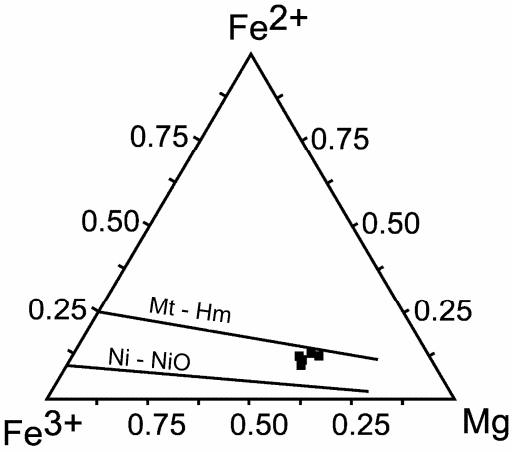

Fig. 15. $Fe^{2+}/Fe^{3+}/Mg$ diagram for biotites with the oxygen fugacity buffers (Wones & Eugster 1965)

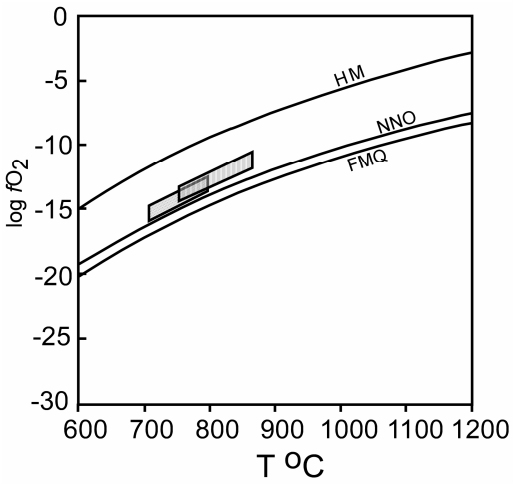

Fig. 16. log fO_2 *vs.* T diagram for the Malko Tarnovo magma. The field with vertical lines reflects the temperature and the oxygen fugacity of monzonitoids, the doted field – for porphyritic rocks of the 4th phase of the pluton

drawn from the biotite composition, but are still indicating oxidising conditions.

An estimation of the water fugacity (f_{H2O}) was made using the biotite–K-feldspar–magnetite association (after Wones & Eugster 1965). The results helped for the estimation of the water contents in melts (Burnham 1979). The method of Burnham et al. (1969) was applied also as independent control. The results (Fig. 17) are 4.0-5.5 wt.% for the monzonitoid melts and 3.5-5.5 wt.% for the melts of the porphyry rocks.

Discussion

Tracing out the magma evolution from the source of melting to the emplacement site where it crystallizes and the fluids are exsolved is important for every attempt to elucidate an ore-magmatic hydrothermal system. The information about the source of melting could be obtained from rocks, formed from melts that have undergone minimum chemical changes after their formation. Volcanic rocks are more felicitous for this purpose, in view of their express transport and short-lived interaction with the crustal rocks. Unfortunately, primitive volcanics are not found in the studied area. We choose some basic rocks (gabbro to monzogabbro) with low strontium isotope ratio ($^{87}Sr/^{86}Sr_i$ =0.7034) indicating weak interaction with the crustal material and having MgO content over 6 wt.% without cumulative structures (Fig. 2, 3 and 6 are used for the selection).

The high contents of the incompatible elements in the gabbro, likely product of the parental magma for the formation of the equigranulare monzonitoids (Fig. 8) support the idea about the metasomatized enriched mantle as a melting source. Spidergrams (Fig. 8) with VHI>HI>MI are explained by Pearce & Parkinson (1993) by weak or moderate melting degree (5-10 %) of FMM (Fertile MORB Mantle). The negative Ti anomaly argued for the presence of a residual amphibole in the mantle source after melting.

Ascribing the negative anomalies of Ti, Ta and Nb to a residual amphibole is unsuitable in our case because amphiboles and phlogopites are the minerals bearing a wide range of trace (mainly incompatible) elements in the enriched mantle. If these minerals were not involved into the melting, hardly the melted magma would be enriched in these incompatible elements.

A number of modern experimental and empirical studies (Münker et al. 2004; Xiong et al. 2005; Bromiley & Redfern 2008) show that rutile has high distribution coefficients (Kd rutile/melt = 2 and 28 for Ta and Nb respectively). The mineral is stable at pressures over 16 kbar, temperatures over 1100°C and water contents below 2 wt.%. Based on the diagram Nb/La *vs.* Zr/Sm it is clear (Fig. 18) that in the particular case just rutile and not amphibole was the residual phase caused the respective negative anomalies. Experimental data for the stability of amphibole (pargasitic amphibole) in mantle conditions are contradictory. They range pressures 18-30 kbar and temperatures 925-1150°C (Niida & Green 1999 and references therein). Most likely the melting temperatures of the mantle source must have not been much higher than 1100°C as the

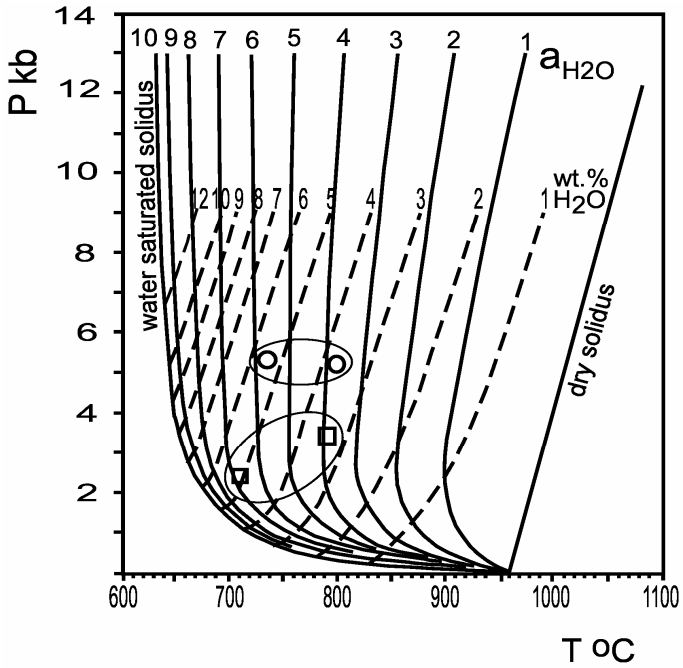

Fig. 17. *P-T* diagram showing solidus curves for a given H_2O activity (a_{H2O}: dashed lines) and liquidus curves (solid lines) for different water contents (Johannes & Holtz 1996). Symbols: (○) quartz-syenites and quartz-monzonites from the 2nd and 3d phases of the pluton; (□) granodiorite and granite porphyries from the 4th plutonic phase

higher temperatures would increase the melting degree, incorporating in the process of melting clinopyroxene, orthopyroxene and olivine. So that, in spite of the incongruent melting of amphibole, following the reaction:

Pargasite = clinopyroxene + olivine + spinel ± melt (Medard et al. 2006), higher temperatures would lead to the decrease of the incompatible elements in the melt. Still higher temperatures would drive to melting of the rutile and not only decrease, but also cause the negative anomalies of Ti, Ta, and Nb to disappear. It seems that the water contents in the mantle rocks might have been lower than 2 wt.% (Fig. 19) as rutile at higher water contents would also have melted when temperatures exceeded 1050°C.

The parental gabbro to monzogabbro magmas generated olivine- and hypersthene-normative (Table 1) rocks. Such parental basic high-K calc-alkaline to transitional (shoshonitic) melts are likely melted products of metasomatized lherzolite or harzburgite, bearing small quantities of phlogopite and pargasite (Conceição & Green 2004). Lherzolites and harzburgites as xenoliths or fragments of ophiolitic complexes are amongst the most often occurring ultramafic rocks in Europe. They had experienced earlier depletion due to the generation of basic magmas (Downes 2002). Later on, they would have been enriched by means of percolation of syn-subduction fluid fluxes and melts. All these conclusions lead to the suggestion that the

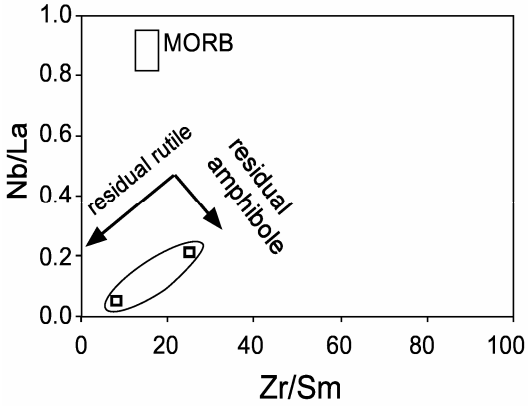

Fig. 18. Nb/La *vs.* Zr/Sm diagram for determination of the residual phase controlling HFSE (Nb, Ta) contents during mantle melting (after Münker et al. 2004). Vectors indicate the tendencies in the values variation of the ratios in the most primitive non cumulative rocks of the association depending on the residual phase (amphibole or rutile)

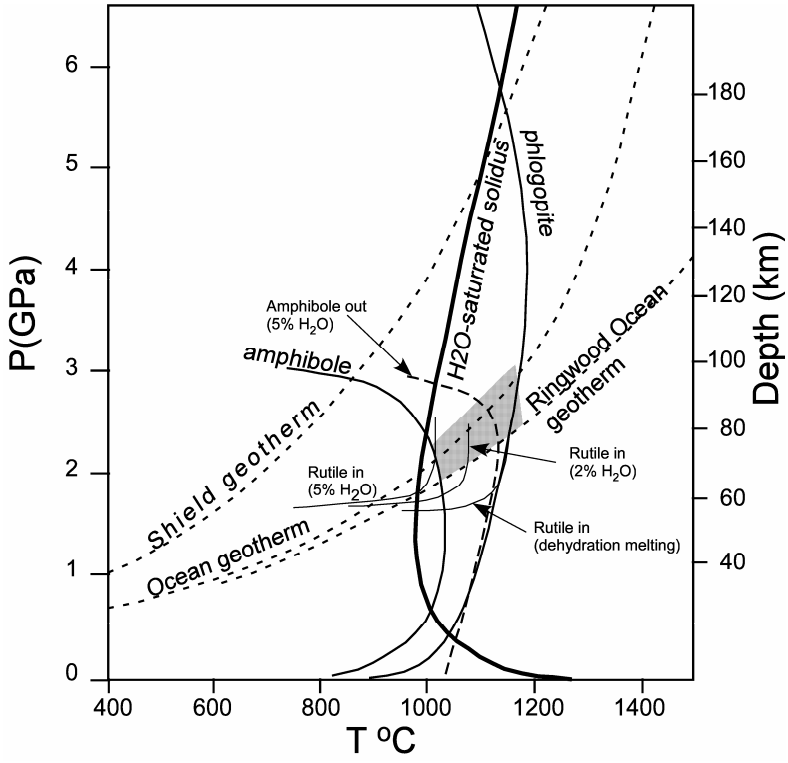

Fig. 19. *P-T* diagram for the H_2O-saturated peridotite melting and stability curves of amphibole and phlogopite (after Wyllie 1979). The dashed curve for the amphibole stability is after Green (1973). The curves for the rutile stability at different water contents in mantle source are after Xiong et al. (2005). Dashed area shows the probable field of melting

Malko Tarnovo magmatic complex is a result of a weak to moderate melting degree of such depleted, but later enriched metasomatized peridotites.

Subsequent evolution of these transitional in alkalinity basic melts depended mainly on the fractionation of predominantly clinopyroxene, less olivine, plagioclase and titanomagnetite. Amphibole and apatite were also included into the fractionating association after monzonitic phase have solidified. Similar evolution leads to increasing of incompatible elements and of the water during its progress.

The crystallization of the monzonitoids had been realized at pressures of 7 to 4 kbar (19-11 km depth). Regardless of the water contents of 4.0-5.5 wt.%, magmas would reach their water saturated state only just at the end of the crystallization process, when they solidified over 70%, according to the investigations of Burnham & Jahns (1962). The extracted water would be little and the relatively high lithostatic pressure would prevent it to get out of the crystallizing magma quickly to higher levels of the Earth crust. It is the very like reason for the rather well expressed skarn aureole around the intrusion to have been formed, due to the prolonged fluidal impact, as well as to the higher temperature gradient at these depths. Fluid degassing probably begin after the formation of the monzonitic phase. This assumption is supported by the decreasing of the concentrations of Cu, Zn, Li, Nb, Y and of the *REE* in the quartz-syenite phase.

The intermediate to acid magma of the porphyry rocks was generated probably in deep crustal levels under the influence of the heat and fluids produced by mantle derived, basic melt, in conformity with the experimental data and the mathematical modeling of Annen et al. (2006). The pure crustal melts, originated by means of melting of metasediments (metagreywackes or metapelites) are dominantly peraluminous, but poor in water and more viscous.

The calc-alkaline magmas that have formed the porphyritic rocks are mainly metaluminous, have low Sr ratio and bimodal distribution of the zircon morphological features with a presence of purely crustal zircon crystals (Fig. 10 and 11 of Kamenov et al. 2006). Evolved residual hydrous mantle-derived magma interacted with newly formed crustal-originated melts to form the magmas of the porphyritic rocks. The melted crustal sources had been metabasites and probably a small amount of metasediments. This kind of crustal melting was accomplished under the influence of hot hydrous basaltic mantle-derived magma and depend on its quantity, repeated intrusions, the depth of the hot zone and the water content (Annen et al. 2006). The inception of such crustal melting may be removed from the pluton by the first portions of basic magma several tens of thousands of years to several millions (3-5 up to 10 Ma) years–"incubation period" (Annen et al. 2006; Jackson et al. 2003). The longer period is typical for crustal melting in relatively shallower and relatively colder levels of the lower crust (between Moho and Conrad) with weaker but prolonged in time basic intrusive magmatism. The Late Cretaceous magmatic activity in Strandzha was relatively weak (compared to the magmatism of Yambol-Burgas volcano-plutonic region of Eastern Srednogorie) and most likely the magma of the porphyry phase, which was relatively time-removed from the previous three phases, had been formed in this way. According to Annen et al. (2006) quartz-dioritic to granodioritic (dacitic to andesitic) melts might be generated when metabasic rocks in the Lower Crust experienced melting degree 20-40%, at temperatures between 900 and 1100°C depending on the water content at the source. The granitoid melt/magma ascend is often more efficient through fractures/dykes for relatively cooler and more viscous magma (Jackson et al. 2003). This ascent mechanism is supported by the dyke-like morphology of the porphyritic bodies of the fourth phase. The calc-alkaline magmas formed the porphyry rocks crystallized at pressures about 3 kbar (8-10 km) and water contents 3.5-5.5 wt.%. Under these circumstances, the magma attained water

saturated condition when 45-48% of its volume had crystallized. This inference is supported also by the petrographical observations. The phenocryst generation (plagioclase, quartz, biotite, amphibole, and K-feldspar) usually constitutes 25-45%. The groundmass, especially in the more densely phenocryst populated varieties, is of leucogranite composition and often exhibits micrographic texture, which is an indication for eutectic crystallization at water saturated conditions. Pressures of about 3 kbar would provoke expansion of some 7-8%, which would cause feebly cracking of the marginal part of the magmatic chamber, as well as of the country rocks (Burnham & Ohmoto 1980). The resulted decompression of the partial residual melt (about 50% of the volume of the whole plutonic body) could release ore-bearing fluids, responsible for the formation of a small to moderate porphyry system, such as the Cu-Mo Bardtse deposit.

Favorable circumstance for generation of the ore-bearing hydrothermal system had been the higher oxidizing conditions (over NNO buffer) of the crystallization and degasing processes. Then only the sulphur had been in oxidized state. Its potential can not be evaluated in the specific case, but obviously facilitated the formation of water-rich fluid and made easier the extracting of the ore components from the melt.

Conclusions

The obtained new geological, petrographical and geochemical data give reasons for the following conclusions about the magma evolution in the Malko Tarnovo magmatic centre and for the genesis of the ore-magmatic systems:

(1) Malko Tarnovo pluton was formed in two stages out of two different in chemistry, structural regimes and crystallization depth melts. During the first stage the isometric and differentiated monzonitoid pluton was formed. It is composed of three phases: (a) gabbroids; (b) monzonitoids; (c) quartz-syenites. The second stage followed some 10 Ma after the monzonitoid stage and includes the granodiorite porphyry phase. Its magmatic bodies are subequatorial elongated and they cut the equigranular monzonitoid ones.

(2) The imperfect separation of clinopyroxene in the first basic phase leaded to the formation of cumulative gabbro to pyroxenite rocks.

(3) The differentiation during the subsequent periods was realized by fractionation of clinopyroxene mainly and titanomagnetite, also plagioclase and olivine to inconsiderable degree. Amphibole and apatite were added to the fractionating association at the end of the monzonitoid magmatism. The mineralogical and geochemical features of the porphyry rocks from the fourth phase, in spite of their narrow extent of differentiation, suggest that the leading role in the fractionation crystallization is assumed for clinopyroxene, magnetite and amphibole and to an insignificant degree–for plagioclase and biotite.

(4) The parental magma of the first three phases was generated by melting of a mantle source of enriched metasomatized rocks. The parental magma of the fourth porphyry phase most probably originated by predominantly melting of metabasic rocks in the Lower Crust, caused by thermal, compositional and infiltration influence of basic and mantle-derived melts.

(5) The crystallized at relatively lower level monzonitoids attained water saturation at higher degree of crystallization (about 70%). The exsolved supercritical fluids are responsible for skarn-formation around the intrusion. In some later stage of the gas-cleaning of the magma, these fluids form the copper mineralization as small massive ore bodies, genetically related to the skarns. The copper extraction out of the first monzonitoid partial magma started after consolidation of the main monzonitoid phase of the pluton.

(6) The cooling and crystallizing porphyritic magma reached earlier its water saturation (after 45% of the melt crystallized). The fluid overpressure provoked fracturation (brecciation) of the porphyritic and the host rocks. The sudden decompression was accompanied with

fluid exsolution and formation of the Cu-Mo small porphyritic system.

(7) Both magmatic-hydrothermal systems in Malko Turnovo centre are substantiated by two geochemically distinct types of mineralizations (polymetallic and W-Mo-polymetallic), noted in the previous studies (Vassileff & Stanischeva-Vassileva 1981, 1986; Ignatovski et al. 1986; Bonev & Yordanov 1983), as well as by two types of ore bodies (ore veins and pillars of massive copper ores, genetically attached to skarns and porphyry type W-Mo-polymetallic, formed at shallower depth).

Acknowledgements: We would like to thank Y. Yanev for the review and the critical comments, helpful for the improvement of the manuscript.

References

Annen C, Blundy J, Sparks R (2006) The genesis of intermediate and silicic magmas in deep crustal hot zones. *Journal of Petrology*, **47**, 505-539.

Aykol A, Tokel S (1991) The geochemistry and tectonic setting of the Demirkoy pluton of the Srednogorie-Istranca granitoid chain, NW Turkey. *Mineralogical Magazine,* **55** (379), 249-256.

Blundy JD, Holland JB (1990) Calcic amphibole equilibria and a new amphibole–plagioclase geothermometer. *Contributions to Mineralogy and Petrology,* **104**, 208-224.

Bogatikov O, Gonshakova V, Borsuk A, Kovalenko V, Kononova V, Lazko E, Sharkov E, Eds. (1983) *Magmatic rocks. Classification, nomenclature, petrography.* Nauka, Moscow, v. 1 and 2, 767 p. (in Russian).

Bogdanov B (1987) *Copper Ore Deposits of Bulgaria*. Techinka Publ. House, Sofia, 388 p. (in Bulgarian with English abstract).

Bonev Il, Yordanov Y (1983) Molybdenum ores in the Bardtze ore deposit, Malko Tarnovo region. In: *First Youth National Workshop in Geology, Sofia 26-28 April 1983, Scientific Reports I, "Geochemistry, Mineralogy, Petrology and Economic Geology"*, 33-41 (in Bulgarian).

Boynton W (1984) Cosmochemistry of the rare earth elements: Meteorite study. In: Henderson P (Editor) *Rare Earth Element Geochemistry*, p. 63-114, Elsevier, Amsterdam.

Bromiiley G, Redfern S (2008) The role of TiO_2 phases during melting of subduction modified crust: Implications for deep mantle melting. *Earth and Planetary Science Letters*, **267**, 301-308.

Brown G, Thorpe R, Webb P (1984) The geochemical characteristics of granitoides in contrasting arcs and comments on magma source. *Journal of the Geological Society of London*, **141**, 413-426.

Burnham CW (1979) The role of volatiles. In: Yoder HSJr (editor), *The Evolution of Igneous Rocks: Fiftieth Anniversary Perspectives*, p. 424-467, Princeton University Press, Princeton.

Burnham C, Jahns R (1962) A method for determining the solubility of water in silicate melts. *American Journal of Science*, **260**, 721-745.

Burnham C, Ohmoto H (1980) Late-stage processes of felsic magmatism. *Mining and Geology, Special Issue*, **8**, 1-11.

Burnham C, Holloway J, Davis N (1969) Thermodynamic properties of water to 1,000^{o}C and 10,000 Bars. *Geological Society of America*, Special Papers, **132**, 96 p.

Chatalov G (1980) Two facies types of Triassic in Strandzha Mountain, SE Bulgaria. *Rivista Italiana di Paleontologia e Stratigrafia*, **85**, 3-4, 1019-1046.

Čatalov G (1983) New data on the age of the rocks of the Veleka group (Strandza Mountain). *Compte Rendus de l'Académie Bulgare des Sciences*, **25**, 11, 927-930.

Chatalov G (1985) Stratigraphy of Strandzha type Triassic sedimentary deposits (Strandzha Mountain, Southeastern Bulgaria). *Geologica Balcanica*, **15**, 6, 3-38 (in Russian with English abstract).

Chatalov G (1990) *Geology of the Strandzha zone in Bulgaria*. Publ. House of the Bulgarian Academy of Sciences, Sofia, 271 p. (in Bulgarian with English abstract).

Cocherie A (1986) Systematic use of trace element distribution on patterns in log–log diagrams. *Geochimca et Cosmochimica Acta*, **50**, 2517-2522.

Conceição R, Green D (2004) Derivation of potassic (shoshonitic) magmas by decom-pression melting of phlogopite+pargasite lherzolite. *Lithos* **72,** 209-229.

Downes H (2002) The lithospheric mantle beneath Central Europe: Evidence from xenoliths. *Geologica Carpathica, Special Issues,* **53**, Proceedings of XVII Congress of CBGA, Bratislava.

Fuhrman M, Lindsley D (1988) Ternary-feldspar modeling and thermometry. *American Mineralogist*, **73**, 201-215.

Green D (1973) Experimental studies on a model Upper mantle composition at high pressure under water-undersaturated and water saturated conditions. *Earth and Planetary Science Letters*, **19**, 37-53.

Ignatovski P, Chobanova A, Bogdanova R (1986) Prognostic estimation and effectiveness of the methodic for searching of the porphyry copper ores in Eastern Srednogorie. *Strandzha-Sakar,* **6**, 107-116 (in Bulgarian with abstract in Russian and English).

Jackson M, Cheadle M, Atherton M (2003) Quantitative modeling of granitic melt generation and segregation in the continental crust. *Journal of Geophysical Research*, **108**, NO. B7, 2332, doi:10.1029/2001JB001050, 23 p.

Johannes W, Holtz F (1996) *Petrogenesis and Experimental Petrology of Granitic Rocks*. Springer, Minerals and Rocks, 335 p.

Johnson MC, Rutherford MJ (1989) Experimental calibration of the aluminium-in-hornblende geobarometer with application to Long Valley caldera (California) volcanic rocks. *Geology*, **17,** 837-841.

Kamenov BK, Tarassova E, Nedyalkov R, Amov B, Monchev P, Mavroudchiev B (2000) New radiometric data from Late Cretaceous plutons in Eastern Srednogorie Area. *Geochimistry, Mineralogy and Petrology*, Sofia, **37**, 13-24.

Kamenov B, Nedyalkov R, Popov M, Tarassova E, Mavroudchiev B (2006) The Malko Tarnovo pluton in Southeastern Bulgaria: I. New data on its petrographical composition and rock forming minerals. *Geochemistry, Mineralogy and Petrology*, Sofia, **44**, 103-130 (in Bulgarian with English abstract).

Le Maitre R (1979) A new generalized petrological mixing model. *Contribution to Mineralogy and Petrology*, **71**, 133-137.

Le Maitre R, Bateman P, Dudek A, Keller J, Lameyre J, Le Bas M, Sabine P, Schmid R, Sorensen H, Strekeizen A, Woolley A, Zanettin B (1989) *A Classification of Igneous Rocks and Glossary of Terms. Recommendations of the International Union of Geological Sciences Subcommissionon the Systematics of Igneous Rocks*, Blackwell, 193 p.

Medard E, Schmidt M, Schiano P, Ottolini L (2006) Melting of amphibole-bearing wehrlits: an experimental study on thre origine of ultra-calcic nepheline-normative melts. *Journal of Petrology,* **47**, 481-504.

Münker C, Wörner G, Yogodzinski G, Churikova T (2004) Behavior of high field strength elements in subduction zones: constraints from Kamchatka–Aleutian arc lavas. *Earth and Planetary Science Letters*, **224**, 275-293.

Niida K, Green D (1999) Stability and chemical composition of pargasitic amphibole in MORB pyrolite under upper mantle conditions. *Contribution to Mineralogy and Petrology*, **135**, 18-40.

Pearce J, Parkinson I (1993) Trace element models for mantle melting: application to volcanic arc petrogenesis. In: Prichard E, Alabaster T, Harris N, Neary C (Editors) *Magmatic Process and Plate Tectonics*, p. 373-403, Geological Society, Special publications, **76**.

Pearce JA, Haris N, Tindle A (1984) Trace element discrimination diagrams for the tectonic interpretation of granitic rocks. *Journal of Petrology,* **25**, 4, 956-983.

Peccerillo A, Taylor S (1976) Geochemistry of Eocene calcalkaline volcanic rocks from the Kastamonon area, Notthern Turkey. *Contribution to Mineralogy and Petrology*, **58**, 63-81.

Pupin JP (1980) Zircon and granite petrology. *Contribution to Mineralogy and Petrology*, **73**, 207-220.

Pupin JP, Turco C (1972) Une typology originale du zircon accessoire. *Bulletin de la Société Française de Minéralogie et Crystallographie*, **95**, 348-395.

Staykov M (1972) Textures of the contact metasomatic ore deposits in the Strandja Anticlinorium. *Proceedings of the Geological Institute, Series Metallic and Nonmetallic Minerals*, **21**, 83-94 (in Bulgarian).

Stewart DB, Wright TL (1974) Al/Si order and symmetry of natural alkali feldspars and the relationship of strained all parameters to bulk composition. *Bulletin de la Société Française de Minéralogie et Crystallographie*, **97**, 356-377.

Sun S, McDonough W, (1989) Chemical and isotopic systematics of ocean basalts: implications for mantle composition and processes. In: Saunders A, Norry M (Editors), *Magmatism in the Ocean Basins*, p. 313-345, Geological Socciety Special Publication.

Vassileff L, Stanisheva-Vassileva G (1981) Metallogeny of the Eurasian copper belt: Sector Bulgaria. *Geologica Balcanica*, **11**, 2, 73-87.

Vassileff L, Stanisheva-Vassileva G (1986) State and problems of the metallogeny of Strandzha-

Sakar. *Strandzha-Sakar ,* **6**, 97-106 (in Bulgarian with abstract in Russian and English).

Vassileff L, Staikov M, Ivanova-Panayotova V, Nechev H (1964) Skarns and ores in the aureole of the Malkov Tarnovo pluton, Strandzha Mountain. In: *Book in Honor of Jovcho Jovchev*, p. 277-348 Techinka Publ. House, Sofia (in Bulgarian with abstract in French).

Wones D (1989) Significance of the assemblage titanite + magnetite + quartz in granitic rocks. *American Mineralogist*, **74**, 744-749.

Wones D, Eugster H (1965) Stability of biotite: Experiment, theory and applications. *American Mineralogist,* **50**, 1228-1272.

Wyllie P (1979) Petrogenesis and the physics of the earth. In: Yoder HS Jr (Editor) *The Evolution of the Igneous Rocks: Fiftieth Anniversary Perspectives*, p. 483-520, Princeton University Press, Princeton.

Xiong X, Adam J, Green T (2005) Rutile stability and rutile/melt HFSE partitioning during partial melting of hydrous basalt: Implications for TTG genesis. *Chemical Geology*, **218**, 339-359.

Accepted April 14, 2009